Structure and stability of small compact self-interstitial clusters in crystalline silicon

Sangheon Lee and Gyeong S. Hwang*
Department of Chemical Engineering, University of Texas, Austin, Texas 78712, USA
(Received 28 June 2007; revised manuscript received 26 October 2007; published 26 February 2008)

We have determined the atomic structure and formation energies of small, compact self-interstitial clusters ($I_n, n \leqslant 10$) in Si using a combination of Metropolis Monte Carlo, tight binding molecular dynamics, and density functional theory calculations. We present predicted local-minimum configurations for compact self-interstitial clusters with $n=5-10$, together with well-defined smaller clusters ($n \leqslant 4$) for comparison. The cluster formation energies per interstitial exhibit strong minima at $n=4$ and 8.

DOI: 10.1103/PhysRevB.77.085210 PACS number(s): 61.72.−y, 66.30.−h

I. INTRODUCTION

Continued scaling of complementary metal oxide semiconductor devices down to the 45 nm design node or beyond will require the formation of ever shallower and more abrupt junctions with higher doping levels. To meet these stringent requirements, it is necessary to have a detailed understanding of the underlying mechanisms of transient enhanced diffusion (TED) and deactivation of implanted dopants during postimplantation annealing. It is now well accepted that the diffusion and clustering of implanted dopants are mainly mediated by native defects created during dopant introduction. In particular, excess Si interstitials are mainly responsible for boron TED and deactivation[1–13] and also play a critical role in TED and clustering of arsenic[1,5,14–20] and phosphorous.[5,19]

Single interstitials are highly mobile even at room temperature.[20] Hence, most interstitials are likely to remain in the form of clusters in bulk Si.[3,4] While extended {311} defects have been well characterized by transmission electron microscopy, earlier spectroscopy measurements based on deep level transition,[21,22] photoluminescence,[22–24] and electron spin resonance[25] have also evidenced the formation of small interstitial clusters (<50 Å in equivalent diameter) at low doses ($10^{12}-10^{14}$ Si/cm^2) and moderate annealing temperatures ($\leqslant$600 °C) before they evolve into larger extended defects with increased ion fluence ($\geqslant 5 \times 10^{13}$ Si/cm^2) and elevated annealing temperatures ($\geqslant$700 °C). In fact, in ultrashallow junction formation with low-energy implanted dopants, small self-interstitial clusters are thought to be a main source for free interstitials responsible for dopant TED and clustering during postimplantation annealing. Therefore, it is necessary to properly describe the agglomeration of Si self-interstitials.

Few attempts have been made to determine the energetics of small interstitial clusters using inverse modeling based on experimental observations of the spatial and temporal concentration variations of interstitial clusters.[26,27] The earlier inverse model studies suggested that there would be a structural transition from compact to elongated forms when the cluster size (n) is around 10 atoms, and also the differential formation energies of small clusters ($n<10$) exhibit two strong minima at $n=4$ and $n=8$. The predictions were also advocated by recent low temperature photoluminescence studies[22–24] which demonstrated possible existence of small and compact interstitial clusters of various sizes. The minimum-energy configurations of a few small clusters ($n=1-5$) have recently been determined using extensive first-principles-based atomistic simulations.[28–32] However, the atomic structure and stability of larger compact interstitial clusters ($n>5$) are uncertain, due partly to their possible complex geometries which might be hard to be determined using first-principles quantum mechanics and tight binding molecular dynamics.

In this paper, we present an effective computational approach to determine the structure and energetics of interstitial clusters, which combines Metropolis Monte Carlo, tight binding molecular dynamics, and first-principles quantum mechanical calculations. Using the approach, we have identified the minimum-energy configurations and formation energies of small, compact self-interstitial clusters ($n \leqslant 10$). The comparison of our work with existing theoretical studies and experimental measurements shows good agreement. Precise determination of the structure and stability of small interstitial clusters will enable more rigorous examinations of temporal and spatial evolutions of interstitial concentration profiles and, in turn, interstitial mediated dopant diffusion and clustering during the formation of ultrashallow junctions in Si-based electronic devices.

II. COMPUTATIONAL APPROACH

Within the continuous random network (CRN) model,[33] a disordered structure is generated via a large number of bond transpositions using Metropolis Monte Carlo (MMC) sampling. The CRN based MMC (CRN-MMC) approach has been successfully used to determine the fully relaxed structure of fully coordinated amorphous materials and their interfaces, while molecular dynamics simulations alone may not always guarantee the construction of thermally equilibrated structures due to their intrinsic time scale limitations. Likewise, we expect that the structure of self-interstitial clusters in Si can also be predicted using CRN-MMC simulations, if all atoms in the clusters are fourfold coordinated. The CRN-MMC approach will certainly be inadequate to determine the structure of defect clusters with a number of coordination defects. According to recent theoretical studies,[30,31] however, the fourfold-coordinate structure of self-interstitial clusters in Si appears energetically favored when they are sufficiently large ($\geqslant 3$). This is apparently due to the fact that the energy gain by bond formation exceeds

the strain energy arising from the fourfold coordination of clusters.

We employed the Keating-like potentials[34] which have been proven to be reliable for studying the relaxed structure of disordered Si materials. Within the Keating-like valence force model, the strain energy (E_{strain}) is defined as

$$E_{strain} = \frac{1}{2}\sum_{i} k_b(b_i - b_0)^2 + \frac{1}{2}\sum_{i,j} k_\theta(\cos\theta_{ij} - \cos\theta_0)^2, \quad (1)$$

where the first and second terms on the right hand side show changes in the strain energy arising from deviations in bond lengths and bond angles, respectively, from their equilibrium values, b_i and b_0 represent the ith bond length and the equilibrium value, respectively, θ_{ij} is the bond angle between bonds i and j to a common atom with the equilibrium value of θ_0, and k_b and k_θ are force constants, respectively, for the two-body and three-body interactions.

The potential parameters were carefully optimized based on gradient corrected density functional theory (DFT) calculations. First, the two-body force constant (k_b) was adjusted to fit DFT values for the total energy variation of crystalline Si with varying amounts of strain (from 10% compressive to 10% tensile). Then, the three-body force constant (k_θ) was adjusted to fit DFT values for the strain energies of five different amorphous Si model structures (of each is within a 64-atom simple cubic cell). Finally, the values for k_b and k_θ were further refined simultaneously based on several interstitial clusters, such as I_4, I_7, and I_8. Through such careful optimization, we have obtained a set of parameters, $k_b = 11.976$ eV/Å^2 and $k_\theta = 2.097$ eV, for DFT values of $b_0 = 2.364$ Å and $\theta_0 = 109.5°$. Note that the optimized parameters are somewhat different from those available in literature ($b_0 = 2.35$ Å, $\theta_0 = 109°$, $k_b = 9.08$ eV/Å^2, and $k_\theta = 3.57$ eV).[34]

Using the CRN-MMC approach, we first determined possible fourfold-coordinate structures for interstitial clusters of different sizes (I_3–I_{10}), starting with various initial configurations for each case. Our in-house CRN-MMC code has been massively parallelized, which allows us to create fairly large interstitial clusters in crystalline Si within a reasonable computation time. The thermal stability of the fourfold-coordinate model structures was carefully checked using high temperature (>1000 K) tight binding molecular dynamics (TBMD) based on highly optimized semiempirical potentials developed by Lenosky *et al.*[35] The structure and energetics of the stable clusters determined by combined CRN-MMC and TBMD simulations were further refined using first-principles calculations based on DFT within the generalized gradient approximation (GGA) of Perdew and Wang (GGA-PW91).[36] While the CRN-MMC, TBMD, or DFT method alone is likely limited to sample all possible cluster configurations, the combined approach has demonstrated to be an effective mean to determine the complex minimum-energy states of small self-interstitial clusters in Si.

All atomic structures and energetics reported herein were calculated using the well established plane wave program VASP (Vienna *ab initio* simulation package).[37] For reference's sake, the formation energies of interstitial clusters were also evaluated within the local density approximation (LDA) by relaxing the GGA structures. For the GGA and LDA calculations, the supercell lattice constants were fixed at 5.460 and 5.382 Å, respectively, as obtained from careful volume optimization. A plane wave cutoff energy of 160 eV was used. Vanderbilt-type ultrasoft pseudopotentials[38] for core-electron interactions were employed, and Brillouin zone sampling was performed using Monkhorst-Pack-type k-point meshes. The mesh size was set to $(2\times2\times2)$ for the 216-atom simple cubic supercell and was properly adjusted with supercell size. For each defect system, all atoms were fully relaxed using the conjugate gradient method until residual forces on constituent atoms become smaller than 5×10^{-2} eV/Å.

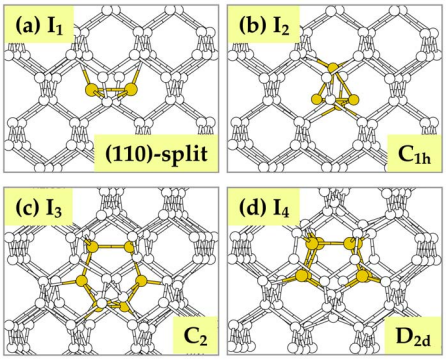

FIG. 1. (Color online) Predicted lowest-energy configurations for (a) I_1, (b) I_2, (c) I_3, and (d) I_4. Gray (gold) balls indicated more distorted atoms than the rest of the lattice atoms (in white). The symmetry for each cluster is also indicated.

III. RESULTS AND DISCUSSION

We first calculated the structure and formation energies of the single and di-interstitials for the sake of reference. As shown in Fig. 1, the ⟨110⟩-split interstitial (I) and the C_{1h} di-interstitial (I_2) turn out to be most stable in the neutral state, with formation energies (per interstitial) of 3.80 and 2.79 eV, respectively. The results are in good agreement with those from previous DFT calculations.[29,30]

It is now well accepted that the tri-interstitial (I_3) and tetrainterstitial (I_4) clusters preferentially form the C_2 and D_{2d} structures, respectively, where all atoms are fourfold coordinated,[30,31] as illustrated in Fig. 1. Our CRN-MMC simulations also predict the ground-state C_2 and D_{2d} configurations. It is also worth emphasizing that the CRN-MMC approach consistently yields the lowest-energy structures, irrespective of the initial position of interstitials as long as they are placed sufficiently close to each other.

For the pentainterstitial (I_5) cluster, the most favorable fourfold-coordinate structure, yet highly distorted while having the trace of I_4, was also determined via the CRN-MMC simulations. During TBMD simulation at 1000 K, indeed the highly strained structure was quickly reconfigured to the more stable I_4+I structure where the fifth interstitial is located near the seven-member ring of the I_4 cluster (see Fig. 2). This implies that such fourfold-coordinate geometry is

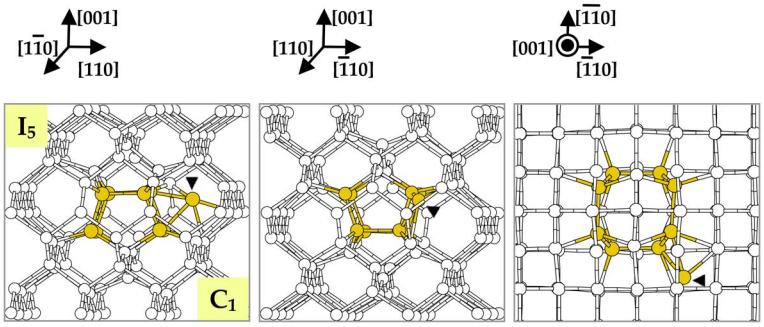

FIG. 2. (Color online) Predicted minimum-energy pentainterstitial (I_5) structure with C_1 symmetry from three different perspectives, as indicated. Gray (gold) balls indicated more distorted atoms than the rest of the lattice atoms (in white), and the fifth interstitial is also indicated.

not thermodynamically favorable. We have also carefully examined other possible local-minimum structures as suggested by earlier modified embedded atom method calculations,[32] such as the structure of I_4+split interstitially. However, they turn out to be at least 0.6 eV less favorable than the I_4+I structure according to our DFT-GGA calculations.

Figure 3 shows a fourfold-coordinate structure of the hexainterstitial (I_6) in which all six interstitials [in gray (gold)] are placed on a (111) plane [referred to as $I_6{}^b$, Fig. 3(b)]. In addition, by introducing two interstitials to the I_4 compact structure, we obtain another I_6 (I_4+2I) structure in which the newly introduced atoms are placed around the seven-member ring of the I_4 cluster [referred to as $I_6{}^c$, Fig. 3(c)]. The fourfold-coordinate $I_6{}^b$ structure is predicted to be as favorable as the $I_6{}^c$ structure, although yielding a highly strained atom (indicated as A). However, combining of the two single interstitials to form a dimer (from $I_6{}^c$) results in a significant lowering of the formation energy, making the combined I_4+I_2 structure to be most favorable energetically [referred to as $I_6{}^a$, Fig. 3(a)].

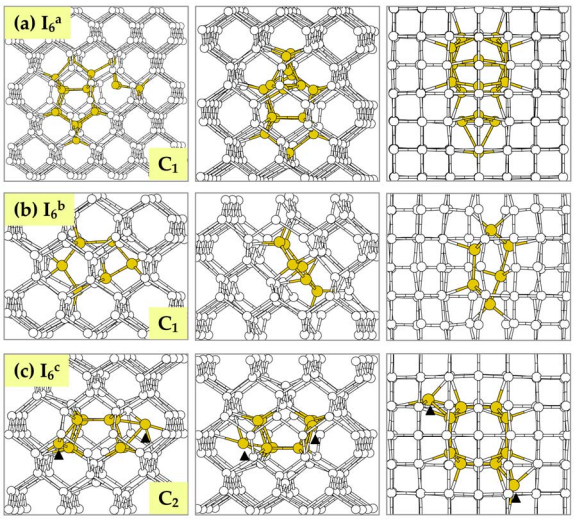

FIG. 3. (Color online) Predicted two nearly degenerate configurations for the hexainterstitial cluster (I_6) from three different perspectives, as indicated (see upper insets in Fig. 2). Gray (gold) balls indicated more distorted atoms than the rest of the lattice atoms (in white). Also, the fifth and sixth interstitials captured by the I_4 cluster are also indicated in (b). The corresponding defect symmetry is indicated.

For the heptainterstitial (I_7) cluster, we have identified three stable fourfold-coordinate structures. The most stable structure [referred to as $I_7{}^a$, Fig. 4(a)] appears a combination of the compact I_4 and I_3 structures which are placed next to each other in the (110) direction. The I_7 structure is predicted to be 0.37 eV more favorable than when the I_4 and I_3 structures are fully separated. Another stable I_7 structure [$I_7{}^b$, Fig. 4(b)] exhibits C_2 symmetry, where two I_3 structures appear linked to each other through an additional interstitial. The center interstitial leads two four-member rings (associated with the I_3 clusters) to two less strained five-membered rings, thereby lowering defect-induced strains. As a result, the $I_7{}^b$ formation energy of 1.94 eV per interstitial is smaller than 2.06 eV for the I_3 cluster. For the third local-minimum structure [$I_7{}^c$, Fig. 4(c)], all seven interstitials are placed on a (111) plane with C_S symmetry, like the $I_6{}^a$ structure. The $I_7{}^b$ and $I_7{}^c$ structures are, respectively, predicted to be 0.39 and 0.75 eV less favorable than the most stable $I_7{}^a$ structure.

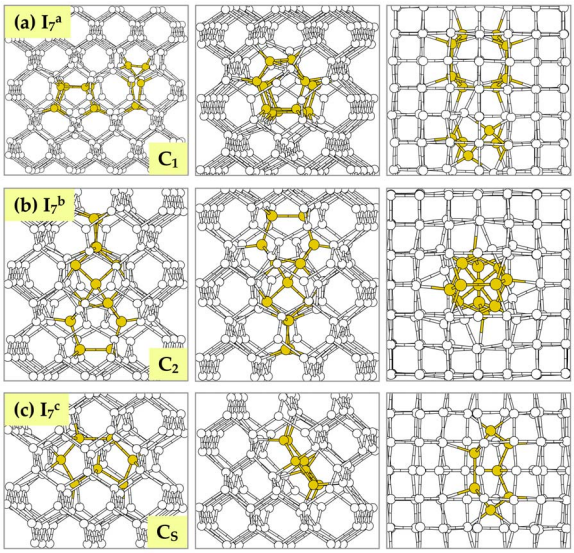

FIG. 4. (Color online) Predicted three local-minimum configurations for the heptainterstitial cluster (I_7) from three different perspectives, as indicated (see upper insets in Fig. 2). The $I_7{}^a$ structure is about 0.39 and 0.75 eV more favorable than the $I_7{}^b$ and $I_7{}^c$ structures, respectively. All structures are fourfold coordinated. Gray (gold) balls indicated more distorted atoms than the rest of the lattice atoms (in white). The corresponding defect symmetries are also indicated.

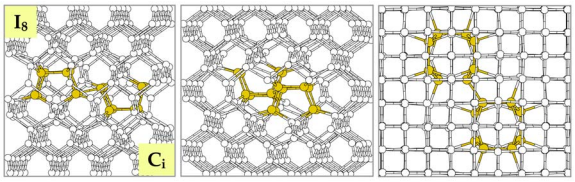

FIG. 5. (Color online) Predicted minimum-energy configuration with C_i symmetry for the octainterstitial cluster from three different perspectives, as indicated (see upper insets in Fig. 2). Gray (gold) balls indicated more distorted atoms than the rest of the lattice atoms (in white).

Our CRN-MMC calculations show that the octainterstitial (I_8) cluster preferentially consists of two stable I_4 clusters as building blocks. Depending on the alignment of the I_4 clusters, several almost degenerate fourfold-coordinate I_8 structures have been determined. Among them, as shown in Fig. 5, the lowest-energy structure exhibits C_2 symmetry, where two I_4 clusters are placed next to each other while having the C_2 rotation axes perpendicular to the (001) plane. The I_8 cluster is likely to lower to some extent the induced strain, relative to two isolated I_4 clusters. The resulting energy gain is estimated to be about 0.3 eV.

For the ennea-interstitial (I_9) cluster, one can first expect a structure [referred to as $I_9{}^a$, Fig. 6(a)] where the ninth interstitial is located around an I_4 seven-member ring of the I_8 cluster, as seen for the I_5 cluster earlier. Indeed, a single interstitial can significantly be stabilized near the I_8 cluster. Unlike the I_5, however, we have also identified a stable fourfold-coordinate structure which is nearly degenerate with the $I_9{}^a$ structure. The highly distorted structure [referred to as $I_9{}^b$, Fig. 6(b)] looks like a combination of two I_4 clusters through an additional interstitial.

Finally, we find that the decainterstitial (I_{10}) cluster preferentially forms a fourfold-coordinate structure. Figure 7 shows two stable fourfold-coordinate I_{10} configurations identified, referred to as $I_{10}{}^a$ and $I_{10}{}^b$, respectively, hereafter. The $I_{10}{}^a$ structure is highly disordered, while the $I_{10}{}^a$ shows C_i symmetry, but the former is predicted to be about 0.3 eV favorable than the latter. Note that in the $I_{10}{}^b$ structure, all ten interstitials are placed on a (111) plane, like in the $I_6{}^b$ and $I_7{}^b$ structures. One might also expect the I_8+2I (or I_2) structure where two single interstitials are trapped around the I_8 cluster, like the I_4+2I (or I_2) cluster. However, the I_8+2I (or I_2) structure turns out to be about 1.7 eV (or 0.1) less favorable than the $I_{10}{}^a$ structure. It is worth noting that the energy gain by bond formation exceeds the energy loss by strain arising from the fourfold coordination as the cluster size increases from I_6 to I_{10}. This is apparently due to more flexibility in the bond rearrangement in the larger cluster.

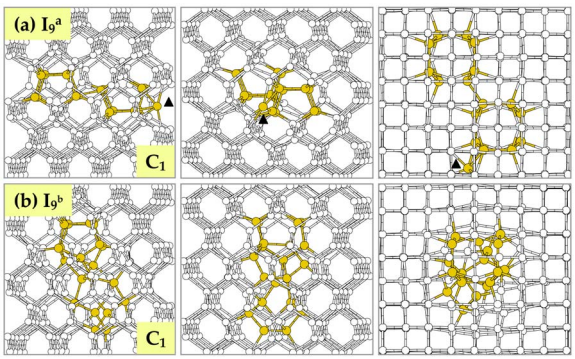

FIG. 6. (Color online) Predicted two local-minimum configurations for the ennea-interstitial cluster (I_9) from three different perspectives, as indicated (see upper insets in Fig. 2). The $I_9{}^a$-structure is about 0.09 eV more favorable than the $I_9{}^b$ structure. In (a), the ninth interstitial captured by the I_8 cluster is indicated. Gray (gold) balls indicated more distorted atoms than the rest of the lattice atoms (in white). The corresponding defect symmetries are also indicated.

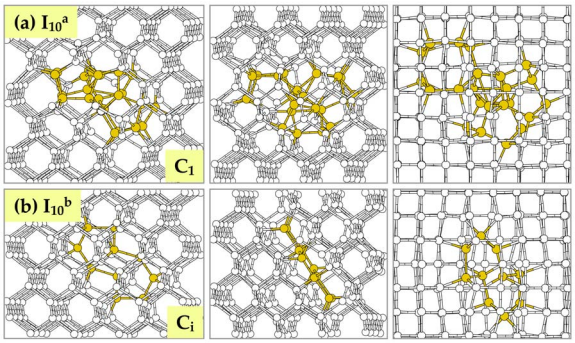

FIG. 7. (Color online) Predicted two local-minimum configurations for the decainterstitial cluster (I_{10}) from three different perspectives, as indicated (see upper insets in Fig. 2). The $I_{10}{}^a$ structure is about 0.3 eV more favorable than the $I_{10}{}^b$ structure. Both structures are fourfold coordinated. Gray (gold) balls indicated more distorted atoms than the rest of the lattice atoms (in white). The corresponding defect symmetries are also indicated.

In Table I, we summarize the formation energies of the small interstitial clusters from our supercell calculations at fixed volumes (as specified) within both the PW91-GGA [see also Fig. 8(a)] and LDA, together with the values attained using the Keating-like (KT) potential model in which parameters were optimized based on DFT-GGA results. As such, the KT and GGA values are in agreement. In addition, particularly for the fourfold-coordinate defect structures, we can see that the GGA and LDA values are very close. In fact, this is not surprising considering that density functional theory generally works well for such simple covalent interactions. Here, the defect formation energy per interstitial $[E_f(n)]$ is given as $E_f(n)=[E(n+N)-(1+n/N)E(N)]/n$, where $E(n+N)$ and $E(N)$ are the total energies of N-atom supercells with a n-interstitial cluster and with no defect. The result clearly demonstrates that by and large the formation energy per interstitial decreases as the number of interstitials increases, as also predicted by earlier studies.[26,27,39] From the result, one can also see that the formation energy variation exhibits a nonmonotonic trend, with strong minima at I_4 and I_8. The results consistent with earlier inverse model studies based on experimental observations,[26,27] which demonstrated that clusters containing four or eight atoms are particularly stable. The oscillating behavior in the stability of small interstitial clusters has also been predicted by other theoretical studies.[40–42]

TABLE I. Predicted values for the formation energies $E_f(n)$ per interstitial of small self-interstitial clusters (I_n, $n=1-10$) from DFT-GGA/LDA and Keating-like potential (KT) calculations as indicated. The supercells α, β, and γ consist of $192+n$, $400+n$, and $480+n$ atoms, respectively, where n is the number of interstitials. The corresponding defect symmetries are also indicated.

Cluster	GGA	(LDA)	KT	Supercell	Symmetry
I_1	3.80	(3.51)	⋯	α	C_{2V}
I_2	2.79	(2.52)	⋯	α	C_S
I_3	2.06	(2.01)	2.45	β	C_2
I_4	1.85	(1.82)	1.81	β	D_{2d}
I_5	2.00	(1.91)	⋯	β	C_1
I_6^a	1.97	(1.87)	⋯	β	C_1
I_6^b	2.09	(2.02)	⋯	β	C_1
I_6^c	2.11	(1.97)	⋯	β	C_2
I_7^a	1.89	(1.88)	2.03	γ	C_1
I_7^b	1.94	(1.91)	1.95	γ	C_2
I_7^c	1.99	(1.96)	1.81	γ	C_S
I_8	1.81	(1.79)	1.74	γ	C_i
I_9^a	1.90	(1.84)	—	γ	C_1
I_9^b	1.91	(1.88)	1.86	γ	C_1
I_{10}^a	1.81	(1.77)	1.84	γ	C_1
I_{10}^b	1.84	(1.80)	1.74	γ	C_i

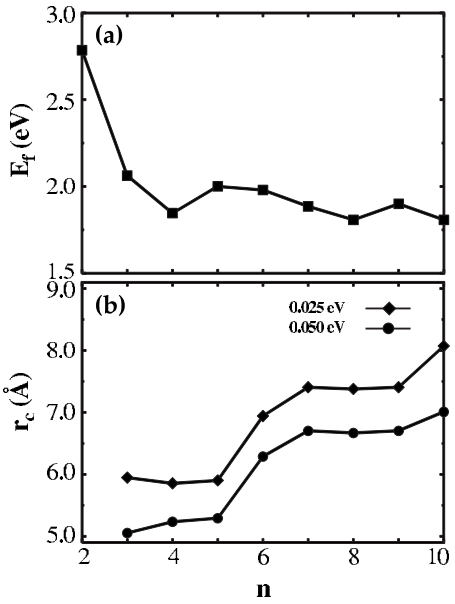

FIG. 8. (a) Predicted formation energies per interstitial E_f of small compact interstitial clusters from our DFT-GGA calculations and (b) their approximate capture radii for mobile interstitials. The capture radius is approximated as $r_c=(3V/4\pi)^{1/3}$, where V is a spherical-like volume that corresponds to the number of Si lattice atoms (excluding interstitials) whose strain energies are greater than a given value (as indicated).

For the identified interstitial clusters, we also estimated their capture radii for mobile interstitials based on the calculation of defect-induced strain fields. For each interstitial cluster, we first counted the number of Si lattice atoms (excluding interstitials) whose strain energies are greater than a given value and then calculated the corresponding volume (V) in bulk Si. This gives a value of capture radius $r_c=(3V/4\pi)^{1/3}$, assuming a spherical volume. We admit that the approach could be oversimplified, but it should be physically sound and sufficient in approximating changes in the capture radius with cluster size, given that the formation energy of interstitials is a function of local strain.[43–45] As summarized in Fig. 8(b), by and large the predicted capture radius increases with cluster size, consistent with earlier inverse model studies.[26,27]

IV. SUMMARY

In this paper, we present an effective computational approach to determine the structure and energetics of compact self-interstitial clusters in Si, which combines CRN model, TBMD, and DFT calculations. For a given defect cluster size, we first constructed possible fourfold-coordinate structures using CRN-MMC simulations, followed by TBMD simulations at high temperatures to check the stability of the fourfold-coordinate structures. Then, DFT calculations were performed to refine the structures of stable defect clusters identified and compared their formation energies to identify minimum energy structures. While the CRN-MMC, TBMD, or DFT method alone would be limited, their combination has been demonstrated to be an efficient mean for determining the lowest-energy configurations of self-interstitial clusters (I_n, $n\geq 3$) in Si, particularly when they prefer fourfold coordination. Using the combined approach, we have identified stable compact structures for self-interstitial clusters with $n=6-10$, along with their formation energies as well as capture radii for mobile interstitials. Our results are consistent with earlier inverse model studies based on experiments. The improved understanding will assist in explaining and predicting the temporal and spatial changes of interstitial concentrations, which is essential for describing interstitial mediated dopant diffusion and clustering in ultrashallow junction formation required for future generations of Si-based electronic devices.

ACKNOWLEDGMENTS

We acknowledge Semiconductor Research Corporation (1413-001), National Science Foundation (CAREER-CTS-0449373), and Robert A. Welch Foundation (F-1535) for their financial support. We would also like to thank the Texas Advanced Computing Center for use of their computing resources.

*Corresponding author. gshwang@che.utexas.edu

[1] P. M. Fahey, P. B. Griffin, and J. D. Plummer, Rev. Mod. Phys. **61**, 289 (1989).
[2] N. E. B. Cowern, K. T. F. Janssen, and H. F. F. Jos, J. Appl. Phys. **68**, 6191 (1990).
[3] D. J. Eaglesham, P. A. Stolk, H.-J. Gossmann, and J. M. Poate, Appl. Phys. Lett. **65**, 2305 (1994).
[4] P. A. Stolk, H.-J. Gossmann, D. J. Eaglesham, D. C. Jacobson, C. S. Rafferty, G. H. Gilmer, M. Jaraíz, J. M. Poate, H. S. Luftman, and T. E. Haynes, J. Appl. Phys. **81**, 6031 (1997).
[5] A. Ural, P. B. Griffin, and J. D. Plummer, J. Appl. Phys. **85**, 6440 (1999).
[6] T. Sinno, H. Susanto, R. A. Brown, W. von Ammon, and E. Dornberger, Appl. Phys. Lett. **75**, 1544 (1999).
[7] W. Luo and P. Clancy, J. Appl. Phys. **89**, 1596 (2001).
[8] C. L. Kuo, W. Luo, and P. Clancy, Mol. Simul. **29**, 577 (2003).
[9] G. S. Hwang and W. A. Goddard, Phys. Rev. Lett. **89**, 055901 (2002).
[10] G. S. Hwang and W. A. Goddard, Appl. Phys. Lett. **83**, 1047 (2003).
[11] G. S. Hwang and W. A. Goddard, Appl. Phys. Lett. **83**, 3501 (2003).
[12] M. Y. L. Jung, R. Gunawan, R. D. Braatz, and E. G. Seebauer, J. Electrochem. Soc. **151**, G1 (2004).
[13] M. Y. L. Jung, C. T. M. Kwok, R. D. Braatz, and E. G. Seebauer, J. Appl. Phys. **97**, 063520 (2005).
[14] S. Solmi, M. Ferri, M. Bersani, D. Giubertoni, and V. Soncini, J. Appl. Phys. **94**, 4950 (2003).
[15] S. A. Harrison, T. F. Edgar, and G. S. Hwang, Appl. Phys. Lett. **87**, 231905 (2005).
[16] S. A. Harrison, T. F. Edgar, and G. S. Hwang, Phys. Rev. B **72**, 195414 (2005).
[17] S. A. Harrison, T. F. Edgar, and G. S. Hwang, Phys. Rev. B **74**, 195202 (2006).
[18] S. A. Harrison, T. F. Edgar, and G. S. Hwang, Electrochem. Solid-State Lett. **9**, G354 (2006).
[19] X.-Y. Liu, W. Windl, K. M. Beardmore, and M. P. Masquelier, Appl. Phys. Lett. **82**, 1839 (2003).
[20] G. D. Watkins, Phys. Rev. B **12**, 5824 (1975).
[21] J. L. Benton, K. Halliburton, S. Libertino, D. J. Eaglesham, and S. Coffa, J. Appl. Phys. **84**, 4749 (1998).
[22] D. C. Schmidt, B. G. Svensson, M. Seibt, C. Jagadish, and G. Davies, J. Appl. Phys. **88**, 2309 (2000).
[23] M. Nakamura and S. Murakami, J. Appl. Phys. **94**, 3075 (2003).
[24] P. K. Giri, Semicond. Sci. Technol. **20**, 638 (2005).
[25] D. Pierreux and A. Stesmans, Phys. Rev. B **71**, 115204 (2005).
[26] N. E. B Cowern, G. Mannino, P. A. Stolk, F. Roozeboom, H. G. A. Huizing, J. G. M. van Berkum, F. Cristiano, A. Claverie, and M. Jaraíz, Phys. Rev. Lett. **82**, 4460 (1999).
[27] C. J. Ortiz, P. Pichler, T. Fühner, F. Cristiano, B. Colombeau, N. E. B. Cowern, and A. Claverie, J. Appl. Phys. **96**, 4866 (2004).
[28] J. Zhu, T. Diaz dela Rubia, L. H. Yang, C. Mailhiot, and G. H. Gilmer, Phys. Rev. B **54**, 4741 (1996).
[29] J. Kim, F. Kirchhoff, W. G. Aulbur, J. W. Wilkins, F. S. Khan, and G. Kresse, Phys. Rev. Lett. **83**, 1990 (1999).
[30] D. A. Richie, J. Kim, S. A. Barr, K. R. A. Hazzard, R. Hennig, and J. W. Wilkins, Phys. Rev. Lett. **92**, 045501 (2004).
[31] N. Arai, S. Takeda, and M. Kohyama, Phys. Rev. Lett. **78**, 4265 (1997).
[32] S. Birner, J. Kim, D. A. Richie, J. W. Wilkins, A. F. Voter, and T. Lenosky, Solid State Commun. **120**, 279 (2001).
[33] F. Wooten, K. Winer, and D. Weaire, Phys. Rev. Lett. **54**, 1392 (1985).
[34] Y. Tu, J. Tersoff, G. Grinstein, and D. Vanderbilt, Phys. Rev. Lett. **81**, 4899 (1998).
[35] T. J. Lenosky, J. D. Kress, I. Kwon, A. F. Voter, B. Edwards, D. F. Richards, S. Yang, and J. B. Adams, Phys. Rev. B **55**, 1528 (1997).
[36] J. P. Perdew and Y. Wang, Phys. Rev. B **45**, 13244 (1992).
[37] G. Kresse and J. Furthmuller, *VASP the Guide* (Vienna University of Technology, Vienna, 2001).
[38] D. Vanderbilt, Phys. Rev. B **41**, 7892 (1990).
[39] J. Kim, F. Kirchhoff, J. W. Wilkins, and F. S. Khan, Phys. Rev. Lett. **84**, 503 (2000).
[40] L. Colombo, Physica B **273-274**, 458 (1999).
[41] M. Gharaibeh, S. K. Estreicher, and P. A. Fedders, Physica B **273-274**, 532 (1999).
[42] M. P. Chichkine, M. M. De Souza, and E. M. Sankara Narayanan, Phys. Rev. Lett. **88**, 085501 (2002).
[43] T. A. Kirichenko, S. K. Banerjee, and G. S. Hwang, Phys. Rev. B **70**, 045321 (2004).
[44] T. A. Kirichenko, S. K. Banerjee, and G. S. Hwang, Phys. Status Solidi B **241**, 2303 (2004).
[45] T. A. Kirichenko, D. Yu, S. K. Banerjee, and G. S. Hwang, Phys. Rev. B **72**, 035345 (2005).